A new technique for estimating the foveal avascular zone dimensions

Agarwal, Arpit, Balaji, J. Jothi, Lakshminarayanan, Vasudevan

Arpit Agarwal, J. Jothi Balaji, Vasudevan Lakshminarayanan, "A new technique for estimating the foveal avascular zone dimensions," Proc. SPIE 11218, Ophthalmic Technologies XXX, 112181R (19 February 2020); doi: 10.1117/12.2543906

SPIE.

Event: SPIE BiOS, 2020, San Francisco, California, United States

A New Technique for Estimating the Foveal Avascular Zone Dimensions.

Arpit Agarwal[*a], J. Jothi Balaji[b], Vasudevan Lakshminarayanan[c]
[a]Department of Chemical Engineering, Indian Institute of Technology, Kanpur 208016, India;
[b] Department of Optometry, Medical Research Foundation, Chennai - 600 006, India
[c]Theoretical and Experimental Epistemology Lab, School of Optometry and Vision Science, University of Waterloo, Waterloo, Ontario N2L 3G1, Canada.

ABSTRACT

The Foveal Avascular Zone (FAZ) is of clinical importance since the vascular arrangement around the fovea changes with disease and refractive state of the eye. Therefore, it is important to segment and quantify the FAZs accurately. Here we provide a new methodology for this measurement. Eighty normal fundus images of dimensions 420x420 pixels corresponding to 6mm x 6mm were used in this study. Each fundus image was manually segmented by a clinical expert (ground truth), the new methodology and an existing technique provided by the image acquisition device (Cirrus 5000 Carl Zeiss Meditec Inc., Dublin, CA). The images were first processed by a Difference of Gaussian (DoG) filter iteratively 25 times after being complemented. This is followed by a Prewitt edge detection and repeated image dilation at angles of 0,45 and 90 degrees. Image closure was then applied followed by noise and small object removal which resulted in the segmented boundary. For deeper insight into shape change, besides the diameter of the FAZ other parameters - eccentricity, perimeter, major axis, minor axis, incircle, circumcircle, F_{min}, F_{max}, tortuosity, vessel diameter index and vessel avascular density - were calculated. The mean diameter by manual segmentation was 673.04 ± 86.92 μm compared to 688.42 ± 72.18 μm by our technique. The corresponding value generated by the instrument was 623.60 ± 121.50 μm. This technique shows considerable improvement in accuracy (the mean value as well as the standard deviation) when compared to system segmentation and the ground truth. These aspects will be discussed in the paper.

Keywords: Image Processing, Foveal Avascular Zone, Optical Coherence Tomography Angiography.

1. INTRODUCTION

Retinal fundus images include the Foveal Avascular Zone (FAZ) which is of clinical importance since the vascular arrangement around the fovea changes depends upon the state of the eye (disease or refractive status). For example, the FAZ size shows a relationship with the severity of Diabetic Retinopathy (DR), one of the major blinding diseases of the eye[1]. High myopia also affects the size and shape of the FAZ[2,3]; Therefore, it is important to segment and quantify the FAZs accurately.

Over the past few decades, advances in technology has provided new platforms for automatic diagnosis in medical settings.[5-9] Major advantage of these advancements has been faster diagnosis and reduction in need of medical specialists. Optical coherence tomography angiography (OCTA) images provide important diagnostic capabilities since they show changes in diabetic and myopic settings.[1,2,3] Only a few studies have been done to segment FAZ automatically. Zheng *et al.*[10] suggested a semi-automatic method to segment FAZ by placing initial contour and moving towards boundary iteratively. They also suggested using a Gaussian kernel to smoothen images. Lu *et al*.[11] suggested automatic FAZ extraction using a snake model and its quantification to classify the images as healthy or diabetic. Diaz *et al.*[12] suggested an automated algorithm to segment FAZ and make use of FAZ area size as a biomarker to study different diseases and the effects of medical treatment. Here we provide a new methodology for this measurement and make comparisons with the ground truth (manual segmentation by a clinical expert). The clinical measurements using this methodology is presented and discussed in a companion paper[4].

* arpitagarwal111@gmail.com

Ophthalmic Technologies XXX, edited by Fabrice Manns, Arthur Ho, Per G. Söderberg, Proc. of SPIE
Vol. 11218, 112181R · © 2020 SPIE · CCC code: 1605-7422/20/$21 · doi: 10.1117/12.2543906

For all the OCTA fundus images used in this study, each FAZ image was segmented by a trained clinician manually, and also by the new methodology. In addition, we used an existing technique provided by the Cirrus 5000 Angioplex [Carl Zeiss Meditec Inc., Dublin, CA] used to capture the images. The segmented boundary was then compared using various shape parameters. Currently comparisons of boundaries are made only on the basis of horizontal and vertical diameter which we believe is not sufficient. Therefore, for deeper insight into shape change, various parameters, such as eccentricity, perimeter, major axis, minor axis, incircle, circumcircle, minimum bounding box (F_{min}), maximum bounding box (F_{max}), orientation of major axis, tortuosity, vessel diameter index (VDI) and vessel avascular density (VAD) were calculated.

2. DATASET

Eighty normal fundus images of dimensions 420x420 pixels corresponding to 6mm x 6mm were used. Age distribution of these images were 37.21 ± 17.09 years. For every image three variants are processed. Non-marked, manually marked and system marked. The new algorithm was applied to non-marked images. The FAZ is the green area in the marked images as shown in (Figure 1). This study was approved by the Institutional Review Board of the Vision Research Foundation, Chennai, India. The study was conducted in accordance with the tenets of the Declaration of Helsinki. Exclusion criteria included any prior history or clinical evidence of retinal or systemic vascular disease. This study was a retrospective chart review of patients who had undergone comprehensive ophthalmic examinations at the Sankara Nethralaya between January 2019 and August 2019.

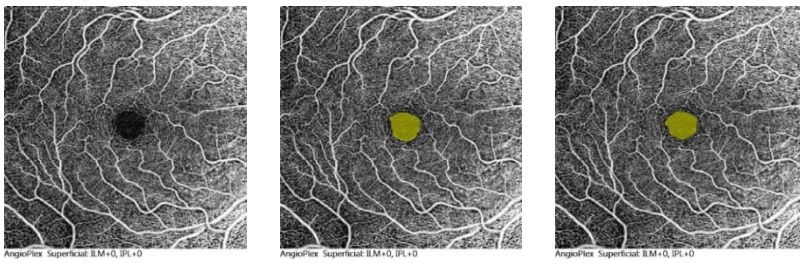

Figure 1. FAZ images: Non-marked (left), manually marked (ground truth; center) and system marked (right).

3. METHODOLOGY

In this study we performed image processing on non-marked images followed by parametric calculations on the detected boundary. The algorithm was implemented in MATLAB *R2016a (Mathworks, Inc.,* Natick, MA). For manually and system marked images only green color FAZ was detected from the images. Using this FAZ region they were also parametrized. This provides a detailed comparison of the new algorithm results with the system algorithm.

3.1 Image Processing

In this new technique, the clear images were segmented by a set of operations shown in the flowchart (Figure 2). Since we need to segment the middle black region from outer vascular region, its important to highlight the difference between the black and white regions. First, the original image was complemented and then a Gaussian filter was used iteratively 25 times.[10] The Gaussian filter is helpful in smoothing and reduces noise. It also intensifies the white FAZ region in comparison to black vessels (figure 2).

The next step removed the vascular structure around the FAZ region. The filtered image was cropped around the center and complemented. Now for edge detection many edge detecting filters are available. In this study we chose the Prewitt edge detector using a threshold value calculated using the Otsu method.[13] Two different threshold values were applied on different parts of the image, and the 25% of thresholding value obtained is applied in a square area around the center consisting of 25% of the image area and a second 55% of the thresholding value was applied to the remaining 75% part. This is because outer area consists of vascular regions which is not of interest. The region inside is of importance and consists of the FAZ. This reduces the number of false positives (which can be clearly seen in Fig 3c) and makes detection

of vascular structure around the FAZs easier. In the current literature, only one value of thresholding is used which is not optimal. We did not use the exact value of the threshold because it results in a large number of false positives.

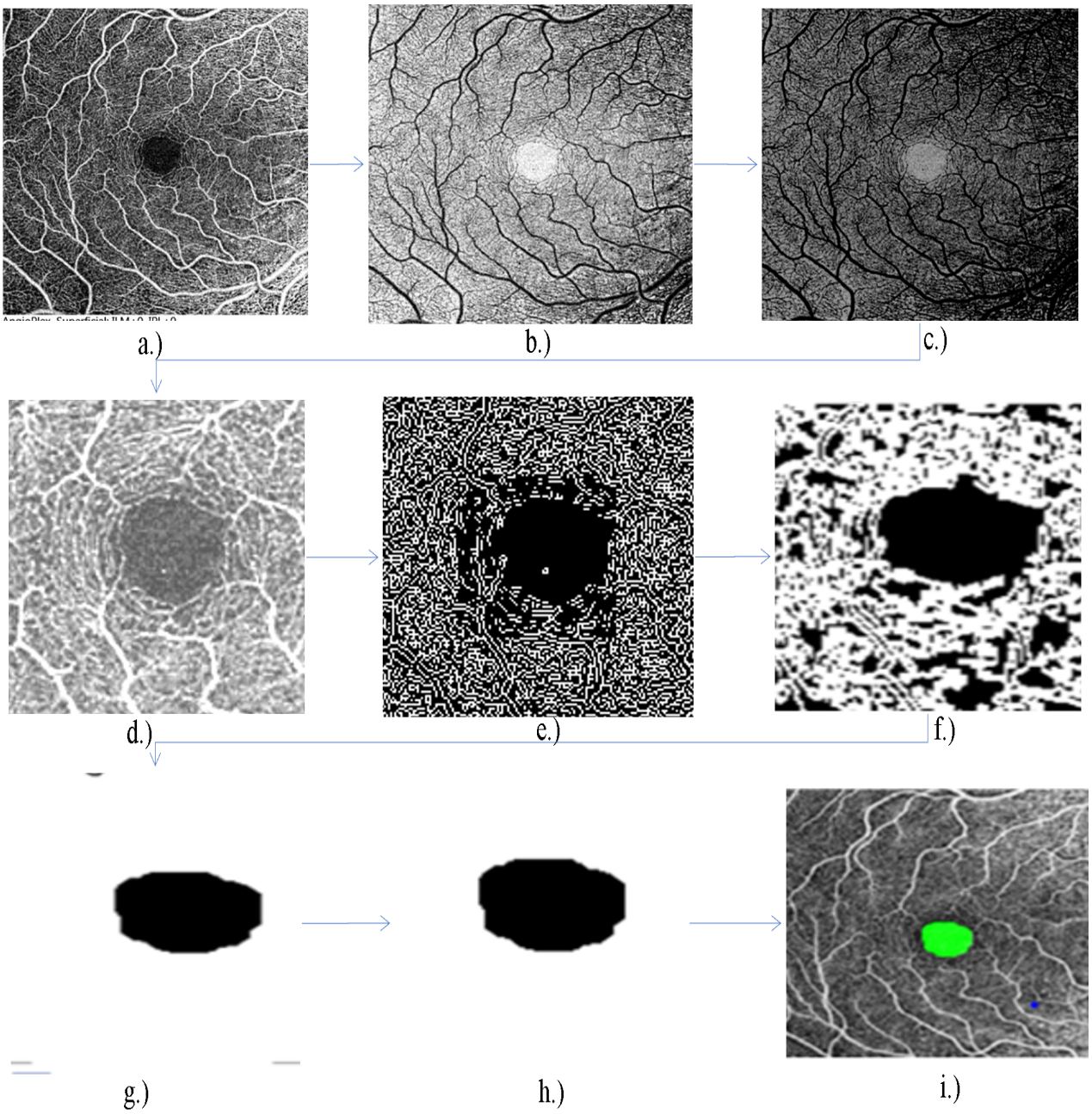

Figure 2. Flow chart illustrating the image processing methodology. a.) Original image b.) Complemented image c.) DoG Filter d.) Complement & crop e.) Prewitt edge detector f.) Image Dilation g.) Image Closure h.) False positive removal & i.) Detected FAZ region.

It is well known that to remove vessel structure, closure is needed which joins all the vessels together.[12] Image closure is a combination of image dilation and erosion. In this study we first dilated the image on angles 0, 45 and 90 degrees using a line shaped element. The angles chosen were equally spaced which helps in maintaining the shape of the FAZs. Image

closure was performed using a disk-shaped element which prevents the curvature of FAZ boundary present. This combination gave better accuracy than using just closure with a disc shaped element.

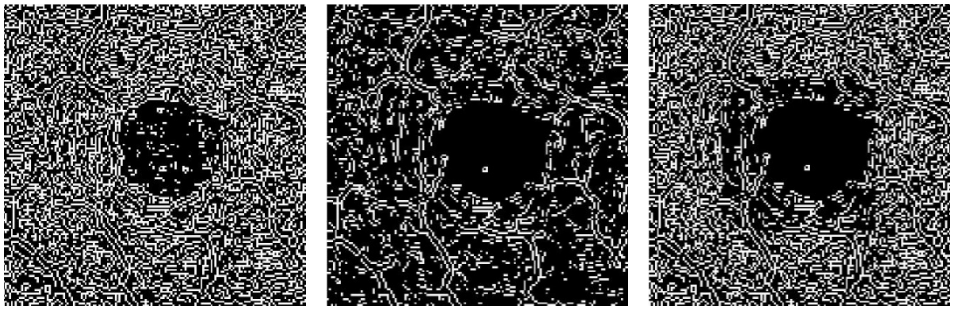

Figure 3. Prewitt edge detector at different thresholds. a.) 55% b.) 25% c.) 55% outside and 25% inside

Now, the FAZ region is clearly segmented but because of the likelihood of false positives, they need to be removed. We selected the biggest of them, since all false positives were found to be considerably smaller than the FAZs during initial tests. This provided the FAZ region of the non-marked image. Next step evaluated parameters using this segmented region and compared with different types of markings.

3.2 Parametric Calculations

In studies conducted to date, the major emphasis has been on the diameter of the FAZ.[14-17] In this paper we present a more robust way to study these boundaries. We suggest the use of thirteen different parameters which describe the boundary. These thirteen parameters are Area, Diameter, Major Axis, Minor Axis, Perimeter, Eccentricity, F_{min}, F_{max}, Inner circle radius, Circumcircle radius, Orientation of the major axis, Tortuosity, Vessel Diameter Index and Vessel Density. Each parameter is explained below:

Area of the FAZ: The area of the green part segmented

Diameter: Corresponding diameter of the circle with same area.

Major axis length: Length (in pixels) of the major axis of the ellipse that has the same normalized second central moments as the FAZ region.

Minor axis length: Minor axis length of the same ellipse.

Perimeter: Length of the FAZ boundary.

Eccentricity: Measure of departure of the region from circularity. For a circular region eccentricity is essentially zero.

F_{min}: Dimension of the smallest side of all rectangles that can contain FAZ totally, with every side of rectangle tangent to the region.

F_{max}: Dimension of the largest side of all rectangles that can contain FAZ totally, with every side of rectangle tangent to the region.

Inner circle radius: The radius of the largest circle that can be inscribed in the FAZ region.

Circumcircle radius: The radius of the smallest circle circumscribing the FAZ region.

Orientation of the major axis: The angle the ellipse makes with the horizontal axis.

Tortuosity: Tortuosity describes the curvature of the curve based on twists and turns. Studies suggest that thickness of curve plays important role in assessing the tortuosity. In ophthalmology it is a diagnostic parameter which is assessed by clinicians based on experience. Method suggested by Trucco *et al.*[18] is used in this study to quantify tortuosity.

Vessel diameter index (VDI): The area occupied by blood vessel from the binarized image over the total length of blood vessel from the skeletonized image.[19] Qualitatively it's the average diameter of all the vessels in the fundus image.

Vessel avascular density (VAD): Area occupied by vessels from the binarized image over the total area of the image. It is basically the density of vessels in the fundus image.[19]

All these parameters are important to study diseased images as they provide a detailed analysis of every aspect of the FAZ boundary as well as region inside it.

4. RESULTS

The mean and standard deviation of all the parameters are listed for all three types of images in Table 1. The new method and the manufacturer's techniques are compared in Table 2. Tortuosity, VAD and VDI are independent of FAZ marking and has to be calculated using non-marked images. Therefore, parameters corresponding to them in system algorithm and manually marked sections are not available.

Table 1. Values of parameters using Proposed method, system algorithm and manually marked images. All values are in μm.

	Proposed method	System algorithm	Manually marked
Diameter (μm)	688.42 ± 72.18	623.60 ± 121.50	673.04 ± 86.92
Major axis (μm)	760.37 ± 95.21	696.50 ± 133.22	740.24 ± 101.29
Minor axis (μm)	637.77 ± 70.24	581.06 ± 120.	625.34 ± 84.20
Perimeter (μm)	2248.34 ± 271.36	2160.44 ± 453.28	2342.54 ± 367.04
Eccentricity (μm)	71.32 ± 24.98	74.16 ± 29.40	75.26 ± 27.16
F_{min} (μm)	634.45 ± 75.09	587.38 ± 122.87	628.06 ± 87.50
F_{max} (μm)	780.40 ± 95.80	732.24 ± 141.22	781.46 ± 111.38
Inner circle radius (μm)	289.36 ± 34.42	261.35 ± 60.25	288.38 ± 39.14
Circumcircle radius (μm)	392.38 ± 47.84	369.20 ± 71.07	392.89 ± 55.52
Orientation (°)	-13.34 ± 43.19	19.00 ± 36.40	-8.63 ± 36.40
Tortuosity (dimensionless**)**	1.45 ± 0.14	_	_
VAD (dimensionless**)**	0.38 ± 0.05	_	_
VDI (μm**)**	26.41± 1.86	_	_

Table 2. Comparison of new algorithm with existing algorithm keeping manual marking as ground truth. Values denote % deviation from manual markings.

	Proposed method	System algorithm
Diameter	2.28%	7.35%
Major axis	2.72%	5.91%
Minor axis	1.99%	7.08%
Perimeter	4.02%	7.77%
Eccentricity	5.23%	1.46%
F_{min}	1.02%	6.48%
F_{max}	0.14%	6.30%
Inner circle radius	0.34%	9.37%
Circumcircle radius	0.13%	6.03%
Orientation	54.57%	320%

5. DISCUSSION & CONCLUSION

The new technique clearly out performs the manufacturer's algorithm. All comparisons are with respect to the ground truth images. In this study we were able to detect boundaries with an error of only 1.99% compared to existing technique with 6.42% error excluding orientation. Orientation of major axis shows 54.57% error with proposed algorithm while 320% error with system algorithm. Clearly there is no confidence in system algorithm for measuring orientation of major axis. One of the major reasons for improved accuracy is due to the new thresholding technique explained in image processing section. It helps in dilating only unnecessary part of the image without distorting the actual FAZ boundary and reduces number of false positive generated. The new combination of dilation and closure provides better results than applying only image closure. The study also provides a new approach to boundary estimation since it parametrizes the boundaries. This

parametrization allows us to provide a holistic comparison of both algorithms. The new algorithm gives better estimates of all parameters except eccentricity. We also find very large accuracies for parameters like F_{max}, Inner circle radius and circumcircle radius. The VDI comes out to be 26.41± 1.86 μm which is greater than the published estimate.[19] This may be because of the difference in number of pixels per unit area in the images. In this study we used 420*420-pixel image corresponding to 6*6-mm. Whereas, the known value was calculated from images of 586*585 pixels corresponding to 3*3-mm. On the other hand, it is well known that vessels tend to become thin with age[20] and this can be one possible reason for the difference in values since the images are not from the same age ranges. This kind of comparison is useful when dealing with different diseases. These comparisons may be useful for diagnosis and classification of different stages or disease states. We believe this robust set of parameters should be evaluated in any FAZ image analysis and comparison. Comparison of these parameters in diseased images is dealt with in the companion paper.[4]

ACKNOWLEDGEMENTS

This work was supported in part by a DISCOVERY grant to V.L. from the Natural Sciences and Engineering Research Council of Canada. None of the authors have any proprietary interest. V.L. is also associated with the Departments of Physics, Electrical and Computer Engineering and Systems Design Engineering.

REFERENCES

[1] Mehta, N., Tsui, E., Lee, G. D., et al., "Imaging Biomarkers in Diabetic Retinopathy and Diabetic Macular Edema." *Int. Ophthalmol. Clinics*, **59(1),** 241-262 (2019).
[2] He, J., Chen, Q., Yin, Y., et al., "Association between retinal microvasculature and optic disc alterations in high myopia." *Eye* **33:** 1494–1503 (2019) doi:10.1038/s41433-019-0438-7.
[3] Gołębiewska, J., Biała-Gosek, K., Czeszyk, A., et al., "Optical coherence tomography angiography of superficial retinal vessel density and foveal avascular zone in myopic children." *PLoS One* 14(7): e0219785. Doi:10.1371/journal.pone.0219785. (2019) (2019).
[4] Jothi Balaji, J.; Agarwal, A.; Raman, R., et al., "Comparison of Foveal Avascular Zone in Diabetic Retinopathy, High Myopia and Normal Fundus images." *Ophthalmic Technologies XXX,* Vol 11218-59. Proc. SPIE (2020).
[5] Novo, J., Hermida, A., Ortega, M., et al., "A Web-Based system enabling computer-aided diagnosis and interdisciplinary expert collaboration for vascular research." *J. Med. Biol. Eng.* **37**: 920-935 (2017).
[6] Novo, J., Rouco, J., Barreira, N., et al., "A web-based system for cardiovascular analysis, diagnosis and treatment." *Comp. Meth. Prog. Biomed.* **139**: 61-81, (2017).
[7] Nishio, M., Nishizawa, M., Sugiyama, O., et al., "Computer-aided diagnosis of lung nodule using gradient tree boosting and Bayesian optimization". *PLoS One* **13(4):**e0195875. Doi: 10.1371/journal.pone.0195875 (2018)
[8] Yanase, J., & Triantaphyllou, E. "A systematic survey of computer-aided diagnosis in medicine: past and present developments." *Expert Systems with Applications*. Doi: 112821. 10.1016/j.eswa.2019.112821. (2019)
[9] Doi, K. "Computer-aided diagnosis in medical imaging: historical review, current status and future potential." *Comp. Med Imag. Graph.* **31(4-5):** 198–211 (2007).
[10] Zheng, Y., Gandhi, J. S., Stangos, A. N., et al., "Automated segmentation of foveal avascular zone in fundus fluorescein angiography." *Invest. Ophthalmol. Vis. Sci,* **51:** 3653-3659. (2010)
[11] Lu, Y., Simonett, J., Wang, J., et. al., "Evaluation of automatically quantified foveal avascular zone metrics for diagnosis of diabetic retinopathy using optical coherence tomography angiography." *Invest. Ophthalmol. Vis. Sci.,* **59:** 2212–2221 (2018).
[12] Dı´az, M., Novo, J., Cutrı´n, P., et. al., "Automatic segmentation of the foveal avascular zone in ophthalmological OCT-A images." *PLoS One* **14(2):** e0212364, doi:10.1371/journal.pone.0195875, (2019).
[13] Yu, C., Dian-ren, C., Yang, Li., et al., "Otsu's thresholding method based on gray level-gradient two-dimensional histogram," *2010 2nd International Asia Conference on Informatics in Control, Automation and Robotics (CAR 2010)*, Wuhan, 2010, pp. 282-285. doi: 10.1109/CAR.2010.5456687

[14] Chui, T. Y. P., Zhong, Z., Song, H., et. al., "Foveal avascular zone and its relationship to foveal pit shape." *Optom. Vis. Sci.* **89**, 602–610 (2012).
[15] Dubis, A. M., Hansen, B. R., Cooper, R. F., et al., "Relationship between the foveal avascular zone and foveal pit morphology." *Investig. Ophthalmol. Vis. Sci.* **53(3)**, 1628–1636 (2012).
[16] Shahlaee, A., Pefkianaki, M., Hsu, J., et al., "Measurement of foveal avascular zone dimensions and its reliability in healthy eyes using optical coherence tomography angiography." *Am. J. Ophthalmol.* **161**, 50-55. e1 (2016).
[17] Choi, J., Kwon, J., Shin JW., et al., Quantitative optical coherence tomography angiography of macular vascular structure and foveal avascular zone in glaucoma. *PLoS One* **12**, 1–19; (2017). Doi: 10.1371/jurnal.pone.0184948
[18] Trucco, E., Azegrouz, H. & Dhillon, B. "Modeling the Tortuosity of Retinal Vessels: Does Caliber Play a Role?" *IEEE Trans. on Biomed. Eng.*, **57**, 2239-47 (2010).
[19] Kim, A. Y., Chu, Z., Shahidzadeh, A., et. al., "Quantifying microvascular density and morphology in diabetic retinopathy using spectral-domain optical coherence tomography angiography." *Invest. Ophthalmol. Vis. Sci*.,**57:** 362–370 (2016).
[20] Sacconi, R., Borrelli, E., Corbelli, E., et al., "Quantitative changes in the ageing choriocapillaris as measured by swept source optical coherence tomography angiography." *Brit. J. Ophthalmol.*, ***103*(9),** 1320-1326 (2019).